Title

YAP/TAZ Regulate Elevation and Bone Formation of the Mouse Secondary Palate

Journal

Journal of Dental Research, 99(12)

ISSN

0022-0345

Authors

Goodwin, AF
Chen, CP
Vo, NT
et al.

Publication Date

2020-11-01

DOI

10.1177/0022034520935372

Peer reviewed

Journal of Dental Research
2020, Vol. 99(12) 1387–1396

DOI: 10.1177/0022034520935372
journals.sagepub.com/home/jdr

YAP/TAZ Regulate Elevation and Bone Formation of the Mouse Secondary Palate

A.F. Goodwin[1,2], C.P. Chen[1,2], N.T. Vo[1,2], J.O. Bush[2,3,4], and O.D. Klein[1,2,4,5]

Abstract

Clefting of the secondary palate is one of the most common congenital anomalies, and the multiple corrective surgeries that individuals with isolated cleft palate undergo are associated with major costs and morbidities. Secondary palate development is a complex, multistep process that includes the elevation of the palatal shelves from a vertical to horizontal position, a process that is not well understood. The Hippo signaling cascade is a mechanosensory pathway that regulates morphogenesis, homeostasis, and regeneration by controlling cell proliferation, apoptosis, and differentiation, primarily via negative regulation of the downstream effectors, Yes-associated protein (YAP) and transcriptional coactivator with PDZ-binding motif (TAZ). We deleted *Yap*/*Taz* throughout the palatal shelf mesenchyme as well as specifically in the posterior palatal shelf mesenchyme, using the *Osr2*^{Cre} and *Col2*^{Cre} drivers, respectively, which resulted in palatal shelf elevation delay and clefting of the secondary palate. In addition, the deletion resulted in undersized bones of the secondary palate. We next determined downstream targets of YAP/TAZ in the posterior palatal shelves, which included *Ibsp* and *Phex*, genes involved in mineralization, and *Loxl4*, which encodes a lysyl oxidase that catalyzes collagen crosslinking. *Ibsp, Phex*, and *Loxl4* were expressed at decreased levels in the ossification region in the posterior palatal shelf mesenchyme upon deletion of *Yap*/*Taz*. Furthermore, collagen levels were decreased specifically in the same region prior to elevation. Thus, our data suggest that YAP/TAZ may regulate collagen crosslinking in the palatal shelf mesenchyme, thus controlling palatal shelf elevation, as well as mineralization of the bones of the secondary palate.

Keywords: palatogenesis, cleft, morphogenesis, mineralization, craniofacial, collagen

Introduction

Clefting of the secondary palate is one of the most common congenital anomalies, with 1/1,700 live births in the United States having isolated cleft palate (Mai et al. 2019). Although modern treatments have improved outcomes, significant morbidities are associated with the standard-of-care interventions for cleft palate, so an improved understanding of palatogenesis is needed. Secondary palate development, which has many similarities between humans and mice, begins when the palatal shelves (PSs) arise from the maxillary processes, grow vertically alongside the tongue, and then reorient into a horizontal position in a process termed PS elevation (Ferguson 1988; Bush and Jiang 2012). The shelves then continue to grow horizontally to meet at the midline and fuse through cellular mechanisms, including apoptosis (Cuervo and Covarrubias 2004; Richardson et al. 2009), as well as intercalation and extrusion of epithelial cells of the medial edge epithelial seam (MES) (Kim et al. 2015). The secondary palate then undergoes ossification.

PS elevation is one of the least understood steps in secondary palatogenesis. In mice, elevation occurs from embryonic day (E) 13.75 to 14.5 (Coleman 1965; Ferguson 1988). Histological studies have suggested that the anterior PSs "flip up" during elevation while the posterior PSs undergo tissue remodeling and protrusion over the tongue (Walker and Fraser 1956; Jin et al. 2010; Yu and Ornitz 2011). Many hypotheses have been proposed for PS elevation, including intrinsic

[1]Department of Orofacial Sciences, University of California, San Francisco, CA, USA
[2]Program in Craniofacial Biology, University of California, San Francisco, CA, USA
[3]Department of Cell and Tissue Biology, University of California, San Francisco, CA, USA
[4]Institute of Human Genetics, University of California, San Francisco, CA, USA
[5]Department of Pediatrics, University of California, San Francisco, CA, USA

A supplemental appendix to this article is available online.

Corresponding Authors:
A.F. Goodwin, Department of Orofacial Sciences, University of California, San Francisco, 513 Parnassus Ave, HSE1506, San Francisco, CA 94143, USA.
Email: alice.goodwin@ucsf.edu
O.D. Klein, Department of Orofacial Sciences, University of California, San Francisco, 513 Parnassus Ave, HSE1508, San Francisco, CA 94143, USA.
Email: ophir.klein@ucsf.edu

factors, such as regional changes in proliferation (Lan et al. 2004; Zhou et al. 2013), alterations in mesenchymal cell density (Brock et al. 2016), and extracellular matrix remodeling (Morris-Wiman and Brinkley 1993; Mansell et al. 2000; Chiquet et al. 2016), including hyaluronic acid accumulation (Brinkley and Morris-Wiman 1987; Lan et al. 2019). Extrinsic factors such as mandibular growth and depression of the mandible and tongue (Ferguson 1977, 1978; Yu and Yonemitsu 2019) and fetal mouth movements (Friedl et al. 2019) have also been invoked. However, a definitive understanding of PS elevation has remained elusive. Later in secondary palatogenesis, the bones of the secondary palate form by intramembranous ossification. The ossification centers are observed as early as E13.5 in the superior region of the PS mesenchyme (Nagata et al. 1991).

Hippo signaling regulates morphogenesis by controlling cellular processes such as proliferation, apoptosis, and differentiation (reviewed in Yu et al. 2015). The cascade functions primarily by negatively regulating its downstream effectors, Yes-associated protein (YAP) and transcriptional coactivator with PDZ-binding motif (TAZ) (Liu et al. 2010; Zhao et al. 2010). Importantly, the Hippo pathway is mechanosensory, in that YAP/TAZ respond to mechanical stimuli (Dupont et al. 2011; Wada et al. 2011) to induce gene transcription via interactions with TEAD DNA-binding proteins (Vassilev et al. 2001; Zhao et al. 2008).

In the craniofacial region, YAP/TAZ play a role in cranial neural crest and mandibular development (Wang et al. 2016), tooth formation (Li et al. 2016), and incisor regeneration (Hu et al. 2017). Of note, loss-of-function mutations in *YAP1* have been reported in families with cleft lip and palate (Williamson et al. 2014). However, the role of YAP/TAZ in secondary palatogenesis has not been reported using animal models.

Here, we interrogated the role of YAP/TAZ in secondary palate development by disrupting their function using multiple Cre drivers in the PS mesenchyme. We found that deletion of *Yap*/*Taz* in the PS mesenchyme caused a consistent delay in PS elevation, which resulted in secondary palate clefting, with reduced bone mineralization, in approximately 30% of embryos. YAP/TAZ have multiple roles in palate formation, including regulating proliferation as well as expression of genes involved in collagen crosslinking and bone mineralization.

Materials and Methods

Mouse Husbandry

All experiments involving mice were conducted in accordance with protocols approved by the UCSF Institutional Animal Care and Use Committee. Mouse lines are listed in Appendix Table 1.

Micro–Computed Tomography

For micro–computed tomography (μCT), E18.5 and postnatal (P) 0 embryo heads were collected and fixed in 4% paraformaldehyde. Samples were scanned using a MicroCT50 (Scanco), 55 kVp, 109 μA, 6 W at a 20-μm voxel size, with a 500-ms integration time and 20.5-mm field of view. Images were analyzed and bone volume and density measured using Avizo software.

Histological Analysis

Timed mating trios were set up, and presence of a vaginal plug was considered E0.5 at noon. Pregnant dams were euthanized and embryos collected and genotyped. For skeletal preparations, skulls were stained with alizarin red and alcian blue and imaged with a Zeiss SteREO Discovery v12, and measurements were taken using Fiji. For other histological analyses, embryonic heads were embedded in paraffin, serially sectioned coronally at 7 μm, and stained with hematoxylin and eosin. Immunohistochemistry was performed using antibodies against YAP (Cell Signaling, #4912, 1:250) and TAZ (Sigma-Aldrich, #HPA007415, 1:100). For proliferation analysis, pregnant dams were injected intraperitoneally with 1 mg BrdU 1 h prior to euthanasia and stained using an antibody against BrdU (Abcam, #6326, 1:500). Nuclei and BrdU-positive cells were quantified using Fiji and statistical significance determined using Student's *t* test. To assess cell death, terminal deoxynucleotidyl transferase-mediated dUTP nick end-labeling (TUNEL) staining (In Situ Cell Death Detection Kit; Roche) was performed. RNAscope (ACD Diagnostics) was performed with mouse probes against *Ibsp, Phex*, and *Loxl4*. Masson staining was performed with the Trichrome Stain Kit (Abcam). Sections were imaged on a Leica DMi8 microscope.

Palatal Shelf Cultures

E13.5 embryos were collected in phosphate-buffered saline (PBS), and the calvarium, mandible, and tongue were removed. Palatal shelf explants were cultured in media (Appendix Table 2) in a rotating culture at 37°C, 50 rpm, and 5% CO_2/95% O_2 for 72 h. Explants were stained with antibody against E-cadherin (Zymed/Invitrogen, #13-1900, 1:250) and imaged on a Zeiss spinning disk microscope.

RNA-Sequencing Experiment

E14.5 embryos were collected, and the position of the PSs, either elevated or nonelevated, was noted. The 2 posterior PSs, posterior and medial to the molar placode, were excised and RNA extraction was performed using the RNeasy Mini Kit (Qiagen, 74104). All samples were of high quality (RNA Quality Number 10). RNA-sequencing (RNA-seq) was performed on an Illumina HiSeq 4000. Read counts were generated, and only mapped reads uniquely assigned to the mouse genome were used for differential expression testing. The expression matrix was imported into R and normalized for sequencing read depth. Quality control plots were created, differential expression was performed using DESeq2 (Wald test), and significant genes were filtered by a threshold of false

discovery rate <0.05,1.5 < $\log_2$FC <–1.0, and raw counts >100. Data were published on GEO (GSE151121).

Results

Deletion of Yap/Taz *throughout the Palatal Shelf Mesenchyme Causes Delayed Elevation and Regional Decreases in Proliferation*

We set out to examine the expression and function of YAP/TAZ in secondary palate development. By immunofluorescence staining, YAP/TAZ were highly expressed in the PS and dental epithelium as well as the PS mesenchyme throughout secondary palate development (Appendix Fig. 1A–F″).

Because YAP/TAZ were highly expressed in the epithelium, we first deleted these genes with the *K14*^{Cre} driver, but we did not observe a phenotype in secondary palatogenesis ($n = 3$, Appendix Fig. 2A–B″). When we deleted *Yap*/*Taz* throughout the PS mesenchyme with the *Osr2*^{Cre} driver, the PSs appeared similar in the *Yap*$^{fl/fl}$;*Taz*$^{fl/fl}$;*Osr2*^{Cre} embryos compared to control at E12.5 and E13.5 (Fig. 1A–D″). However, by E14.5, while the control PSs elevated, all mutant PSs were still in the vertical orientation (Fig. 1E–F″). Of note, we recovered no *Yap*$^{fl/fl}$;*Taz*$^{fl/fl}$;*Osr2*^{Cre} embryos later than E14.5 ($n = 8$ litters), and fewer mutants than expected (1/8 = 12.5%, according to our breeding scheme) were recovered at earlier stages (8 mutants out of 103 collected = 7.8% at E12.5, 8/129 = 6.2% at E13.5, and 8/106 = 7.5% at E14.5), indicating embryonic lethality. *Yap*$^{fl/fl}$;*Taz*$^{fl/fl}$;*Osr2*^{Cre} embryos had lesions filled with blood in the mandible and limbs at E13.5 and E14.5 (Appendix Fig. 3A–F′).

Yap$^{fl/fl}$;*Taz*$^{fl/+}$;*Osr2*^{Cre} compound mutant embryos had a similar elevation delay and did not survive past E14.5. However, we were able to collect more of these than *Yap*$^{fl/fl}$; *Taz*$^{fl/fl}$;*Osr2*^{Cre} embryos at E14.5, and we quantified the elevation delay using this model. We staged these embryos precisely into developmental substages, as in Geyer et al. (2017). At stage 23, all of the control embryos had PSs that were adhered or fused (n = 4/9 = 44% and n = 5/9 = 56%, respectively), whereas all of the mutant embryos were either in the vertical (n = 1/3 = 33%) or horizontal position (n = 2/3 = 67%), and none were adhered or fused. Thus, deletion of *Yap*/*Taz* throughout the PS mesenchyme resulted in a significant and consistent delay in PS elevation.

We next investigated if there were differences in cell proliferation and death in the PS mesenchyme with deletion of *Yap*/*Taz*. At E12.5, when the PSs are undergoing significant growth, there was a decrease in proliferation of 8% in the posterior PS mesenchyme in the *Yap*$^{fl/fl}$;*Taz*$^{fl/fl}$;*Osr2*^{Cre} embryos compared to control (Fig. 1H–J, $n = 5$). Apoptosis was extremely low in the PS mesenchyme at E12.5, with only 1% of the total cells in this region staining positive for TUNEL (data not shown), suggesting apoptosis is unlikely a major contributor to the PS elevation delay. However, the regional decrease in proliferation that we identified could contribute to the observed PS elevation delay.

Deletion of Yap/Taz *Specifically in the Posterior Palatal Shelf Mesenchyme Results in Elevation Delay and Clefting of the Secondary Palate*

Because of the high incidence of embryonic lethality with vascular defects upon deletion of *Yap*/*Taz* with *Osr2*^{Cre}, it was not feasible to collect enough samples for further mechanistic studies, and so we sought an alternative PS mesenchymal Cre driver for further study. *Col2*^{Cre} drives recombination in multiple tissues such as cartilage of the long bones and skull, including Meckel's cartilage. We found that, in addition, *Col2*^{Cre} drives recombination in a subset of mesenchymal cells in the posterior palate as early as E12.5 (Appendix Fig. 4A–D″). To avoid embryonic lethality and delete *Yap*/*Taz* in the posterior PS mesenchyme, where we observed decreased proliferation, we used *Col2*^{Cre}. *Yap*$^{fl/fl}$;*Taz*$^{fl/fl}$ littermate controls had fused palates, whereas approximately 30% (n = 8/26) of the *Yap*$^{fl/fl}$;*Taz*$^{fl/fl}$;*Col2*^{Cre} mutant pups had a complete cleft of the secondary palate at P0 (Fig. 2A, B). μCT at P0 showed that the bones of the control were fused to form a continuous secondary palate (Fig. 2C), whereas there was a wide gap between the palatine processes of the maxillary and palatine bones in the *Yap*$^{fl/fl}$;*Taz*$^{fl/fl}$;*Col2*^{Cre} mutant (Fig. 2D).

At E13.5, the size and shape of the *Yap*$^{fl/fl}$;*Taz*$^{fl/fl}$;*Col2*^{Cre} PSs appeared similar to control (Fig. 2F–G″). However, by E14.5, when PSs in control embryos elevated into the horizontal position, the PSs in *Yap*$^{fl/fl}$;*Taz*$^{fl/fl}$;*Col2*^{Cre} embryos remained in the vertical position (Fig. 2H–I″). By E15.5, the control PSs were adhered and undergoing fusion, with degeneration of the MES under way, but the *Yap*$^{fl/fl}$;*Taz*$^{fl/fl}$;*Col2*^{Cre} PSs were just beginning to elevate (Fig. 2J–K″). We quantified the PS elevation delay in staged E14.5 *Yap*$^{fl/fl}$;*Taz*$^{fl/fl}$;*Col2*^{Cre} embryos and found it was consistent (Fig. 2E). Of the *Yap*$^{fl/fl}$;*Taz*$^{fl/fl}$;*Col2*^{Cre} embryos examined at E12.5 (n = 7), E13.5 (n = 5), and E14.5 (n = 4), there was no significant difference in proliferation (Appendix Fig. 5), although this could be attributable to the expression of the *Col2*^{Cre} in a subset of PS mesenchymal cells and low penetrance of the clefting phenotype in this model.

The Elevation Defect Due to Loss of Yap/Taz *Is Intrinsic to the Palatal Shelves and Does Not Involve the Mandible*

Previous studies have demonstrated that aberrant mandibular size or position may prevent PS elevation (Dudas et al. 2004; Huang et al. 2008; Parada et al. 2015). *Col2*^{Cre} drives recombination in Meckel's cartilage, and we wanted to determine whether deletion of *Yap*/*Taz* disrupted PS elevation indirectly through effects on the mandible. We first examined the size and shape of the mandible and cranium in skeletal preparations at E18.5 and found that these were the same across control and mutant, with the exception of a statistically significant but small (4%) increase in cranial width in the mutant (Fig. 3A, B, n = 8 controls and 8 mutants, 1 with cleft, 7 without cleft). Using μCT, we measured the skulls of *Yap*$^{fl/fl}$;*Taz*$^{fl/fl}$ controls (n = 4) and *Yap*$^{fl/fl}$;*Taz*$^{fl/fl}$;*Col2*^{Cre} embryos with clefts (n = 3)

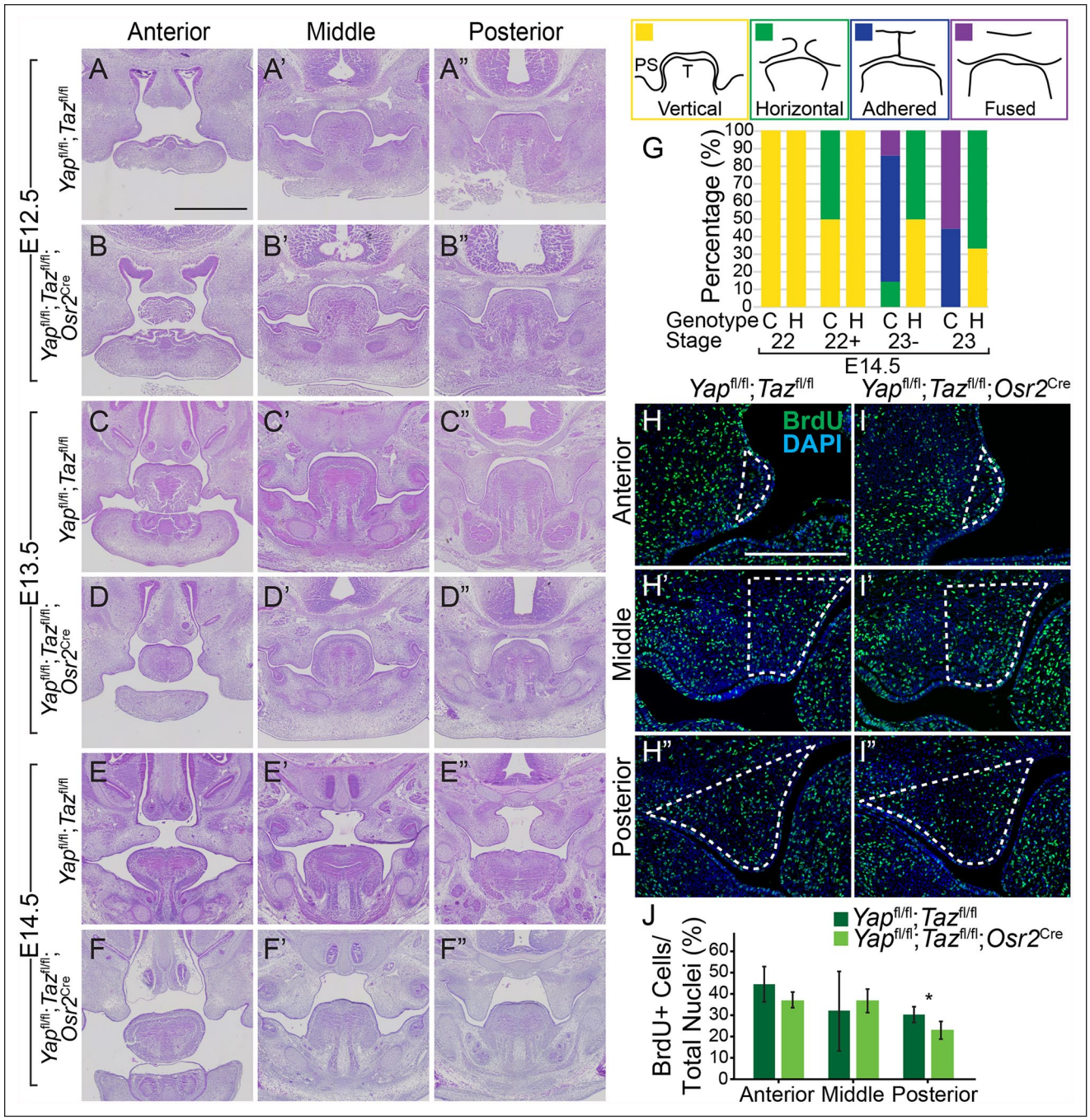

Figure 1. Deletion of *Yap*/*Taz* throughout the palatal mesenchyme causes elevation delay and decreased proliferation. (**A–F″**) Images of hematoxylin and eosin (H&E) staining show $Yap^{fl/fl}$;$Taz^{fl/fl}$ control and $Yap^{fl/fl}$;$Taz^{fl/fl}$;$Osr2^{Cre}$ mutant embryo palatal shelves appeared similar in size and shape at E12.5 (A–B″) and E13.5 (C–D″), but by E14.5, while the control palatal shelves elevated (E–E″), the mutant palatal shelves were in the vertical position (F–F″). Scale bar = 1 mm. (**G**) Schematic showing the vertical, horizontal, adhered, or fused position of the palatal shelves (PSs) relative to the tongue (T) and graph of the percentage of palatal shelves in each position at each Theiler stage in the $Yap^{fl/fl}$;$Taz^{fl/fl}$ control (C) and $Yap^{fl/fl}$;$Taz^{fl/+}$;$Osr2^{Cre}$ compound heterozygous (H) embryos. Number of embryos examined at each Theiler stage: n = 4 controls and 2 heterozygotes at 22, 2 controls and 7 heterozygotes at 22+, 7 controls and 4 heterozygotes at 23–, and 9 controls and 3 heterozygotes at 23. (**H**, **I″**) Immunofluorescence with antibody against BrdU (green) and DAPI (blue) staining in the anterior (H, I), middle (H′, I′), and posterior (H″, I″) in $Yap^{fl/fl}$;$Taz^{fl/fl}$ control and $Yap^{fl/fl}$;$Taz^{fl/fl}$;$Osr2^{Cre}$ mutant embryos at E12.5 with the region of the palatal shelf mesenchyme quantified outlined by the white dashed lines. Scale bar = 50 µm. (**J**) Quantification of percent BrdU-positive cells in the palatal shelf mesenchyme revealed a significant 8% decrease in proliferation in the posterior palatal shelf mesenchyme of the $Yap^{fl/fl}$;$Taz^{fl/fl}$;$Osr2^{Cre}$ mutant compared to control. *P = 0.02.

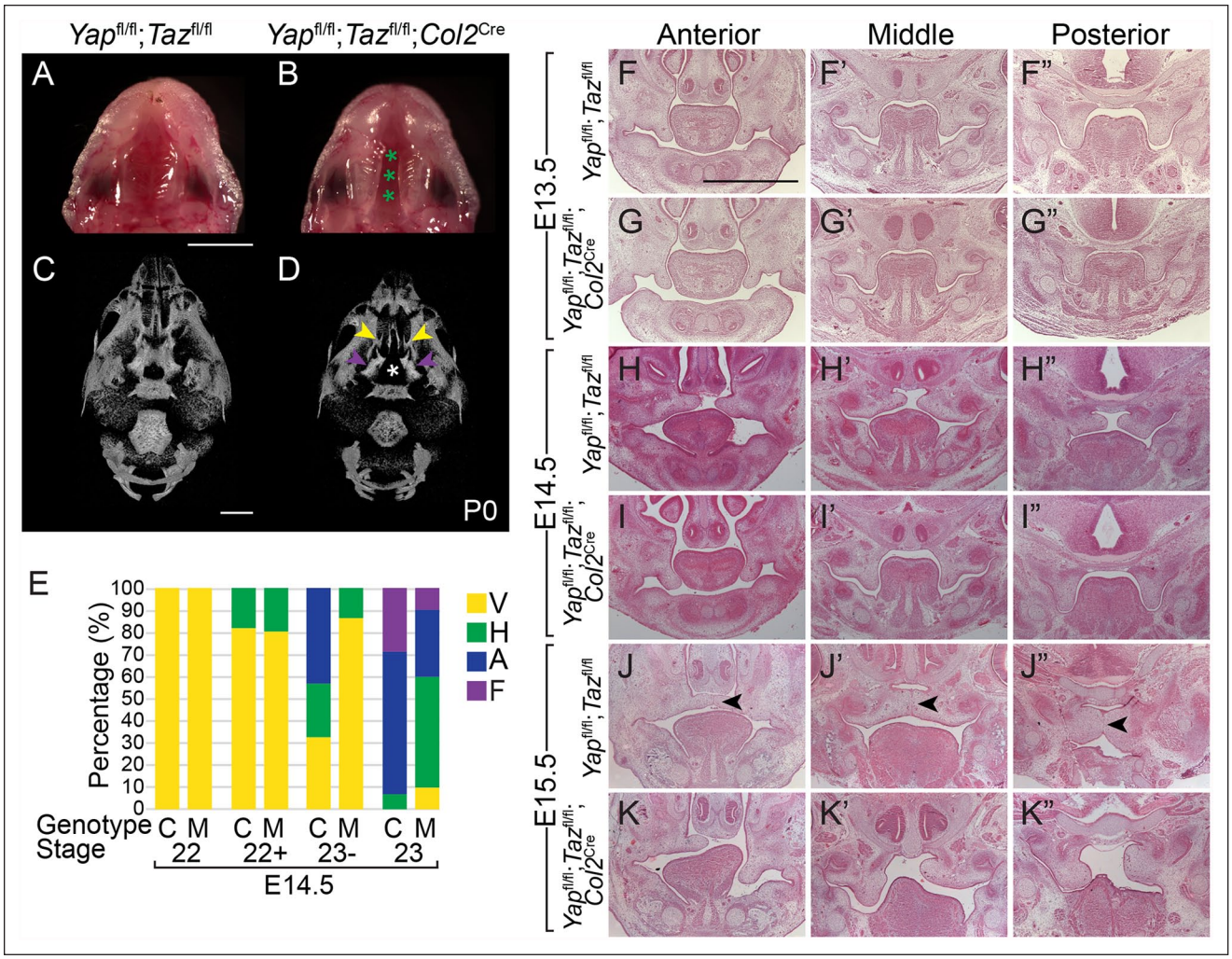

Figure 2. Deletion of *Yap*/*Taz* in the posterior palatal shelf mesenchyme results in elevation delay and clefting of the secondary palate. (**A, B**) Images of the ventral view of the palate at P0 show the normal fused palate in the *Yap*$^{fl/fl}$;*Taz*$^{fl/fl}$ control and a complete cleft of the secondary palate in the *Yap*$^{fl/fl}$;*Taz*$^{fl/fl}$;*Col2*^{Cre} mutant embryo (demarcated with green asterisks). Scale bar = 1 mm. (**C, D**) Ventral views of 3-dimensional renderings of micro–computed tomography data at P0 show that while the maxillary and palatine bones that form the secondary palate were fused in the *Yap*$^{fl/fl}$;*Taz*$^{fl/fl}$ control embryo (C), the palatine process of the maxillary (yellow arrows) and palatine (purple arrows) bones was undersized and separated by a cleft (white asterisk) in the *Yap*$^{fl/fl}$;*Taz*$^{fl/fl}$;*Col2*^{Cre} embryo (D). Scale bar = 1 mm. (**E**) Graph of the percentage of palatal shelves in the vertical (V), horizontal (H), adhered (A), or fused (F) position at each Theiler stage in the *Yap*$^{fl/fl}$;*Taz*$^{fl/fl}$ control (C) and *Yap*$^{fl/fl}$;*Taz*$^{fl/fl}$;*Col2*^{Cre} mutant (M) embryos. Number of embryos examined at each Theiler stage: $n = 4$ controls and 3 mutants at 22, 11 controls and 5 mutants at 22+, 37 controls and 29 mutants at 23–, and 14 controls and 10 mutants at 23. (**F–K″**) Images of hematoxylin and eosin staining show *Yap*$^{fl/fl}$;*Taz*$^{fl/fl}$ control and *Yap*$^{fl/fl}$;*Taz*$^{fl/fl}$;*Col2*^{Cre} mutant embryo palatal shelves appeared similar in size and shape at E13.5 (F–G″). While control palatal shelves elevated by E14.5, the mutant palatal shelves remained in the vertical position (H–I″), and at E15.5, the control palate was undergoing fusion with the medial epithelial seam in the process of degeneration (black arrows) while the mutant palatal shelves were elevating (J–K″). Scale = 1 mm.

and without clefts ($n = 2$) at E18.5 and found a statistically significant decrease in the cranial base and maxilla length in the *Yap*$^{fl/fl}$;*Taz*$^{fl/fl}$;*Col2*^{Cre} embryos with clefts (Appendix Fig. 6A, B). In addition, there was a small but statistically significant decrease ($P = 0.04$) in the condylar process width in mutant embryos with clefts, but there were no differences in any of the other measurements of the mandible (Appendix Fig. 6A, B). Thus, 2 different approaches to measuring the mandible showed that deletion of *Yap*/*Taz* with the *Col2*^{Cre} driver did not affect mandibular development.

In other mutants in which the mandible prevented elevation, its removal in culture could rescue PS elevation (Huang et al. 2008; Parada et al. 2015). We cultured whole maxillae with mandibles removed from E13.5 embryos (Shiota et al. 1990). This culture system tests the ability of palatal shelves to elevate and grow toward the midline and is distinct from trowel-type palatal shelf explant cultures, which specifically assay secondary palate fusion (Brunet et al. 1993). In the majority of control explanted maxillae, PSs elevated and adhered and only 33% failed to do so (2/6); however, most of the *Yap*$^{fl/fl}$;*Taz*$^{fl/fl}$;*Col2*^{Cre} mutant explants did not fuse (5/7; 71%; Fig. 3C–E). Previous reports using similar protocols have shown clefting in control explant cultures at ~19% (Huang et al. 2008). Therefore, removal of the mandible did not rescue cleft palate in

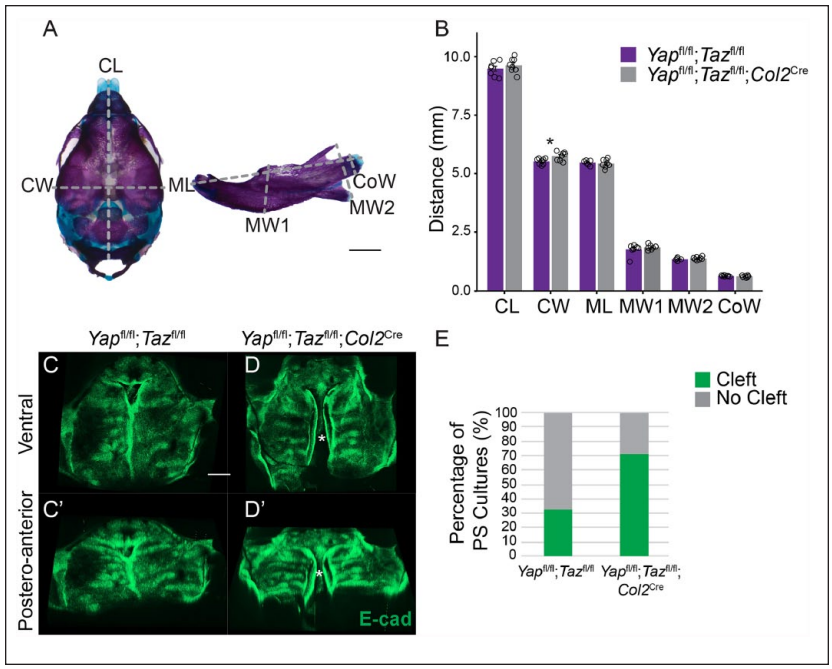

Figure 3. The elevation defect due to mesenchymal loss of *Yap*/*Taz* is intrinsic to the palatal shelves and does not involve the mandible. (**A**) Images of E18.5 skeletal prep-stained skull and mandible with dimensions analyzed marked with dashed gray lines. Scale bar = 1 mm. CL, cranium length; CoW, condylar width; CW, cranium width; ML, mandibular length; MW1, mandibular width 1; MW2, mandibular width 2. (**B**) Graph of measurements of dimensions demarcated in A. Note that there was only a significant difference in the cranial width and not mandibular size and shape in $Yap^{fl/fl};Taz^{fl/fl}$ control and $Yap^{fl/fl};Taz^{fl/fl};Col2^{Cre}$ mutant embryos (*$P = 0.04$). (**C–D′**) Representative images of E-cad-stained palatal shelf explants imaged from the ventral (C, D) and posteroanterior (C′, D′) aspect. Note that while the majority of $Yap^{fl/fl};Taz^{fl/fl}$ control explants elevated and adhered in culture and did not have a cleft, most $Yap^{fl/fl};Taz^{fl/fl};Col2^{Cre}$ mutant explants elevated but did not fuse, resulting in a visible cleft (marked by asterisk). (**E**) Quantification of the percentage of palatal shelf explants with or without clefts after 72 h in culture.

$Yap^{fl/fl};Taz^{fl/fl};Col2^{Cre}$ mutants, indicating that the cleft secondary palate phenotype was not due to effects on the mandible but more likely due to intrinsic PS defects.

Loss of Yap/Taz *in the Palatal Shelf Mesenchyme Results in Disruption of Mineralization of the Bones of the Secondary Palate*

Given the elevated expression of YAP/TAZ in the osteogenic centers of the PSs (Appendix Fig. 1C″), we asked whether *Yap*/*Taz* deletion affected secondary palate bone formation later in development. We measured the volume and density of the bones of the secondary palate by μCT of $Yap^{fl/fl};Taz^{fl/fl}$ control and $Yap^{fl/fl};Taz^{fl/fl};Col2^{Cre}$ mutant embryos with and without clefts at E18.5. Compared to control, the bone volume of the palatine processes of the maxillary and palatine bones was significantly decreased in mutants with cleft but not in those without cleft (Fig. 4A–H), without a significant difference in the relative bone mineral density (Fig. 4I). We also measured the bone volume and density of the basioccipital and basisphenoid bones, which undergo endochondral ossification and express $Col2^{Cre}$, and found no difference in bone volume, but there was a significant decrease in the density of the basioccipital bone in the $Yap^{fl/fl};Taz^{fl/fl};Col2^{Cre}$ embryos with clefts (Appendix Fig. 7A–E). Thus, deletion of *Yap*/*Taz* in the PS mesenchyme resulted in smaller secondary palate bones and reduced bone mineralization in endochondral bones.

YAP/TAZ Regulate Genes Necessary for Elevation and Mineralization in the Palatal Shelves

To determine which genes YAP/TAZ regulate to impact PS elevation, we performed RNA-seq on nonelevated posterior PSs from TS23– $Yap^{fl/fl};Taz^{fl/fl};Col2^{Cre}$ mutant and control embryos (Appendix Fig. 4A″). We found 6 differentially expressed genes that met the criteria (false discovery rate <0.05, $1.5 < \log_2 FC < -1.0$, and raw counts >100; Appendix Table 3); the 3 most differentially expressed genes, *Ibsp, Phex*, and *Loxl4*, all with decreased expression in the $Yap^{fl/fl};Taz^{fl/fl};Col2^{Cre}$ mutant embryos compared to control, are involved in skeletal development. *Ibsp*, which encodes a major protein component of bone, was specifically expressed in the posterior, but not anterior and middle, PSs at TS23– (Fig. 5B–C′). In the palate, *Ibsp* expression was specific to the ossification center in the posterior PS, and the expression domain and level were decreased in the $Yap^{fl/fl};Taz^{fl/fl};Col2^{Cre}$ embryos compared to control (Fig. 5B′, C′). Similarly, *Phex*, which encodes an enzyme involved in mineralization, was expressed in the mineralizing mandible (Fig. 5D, E) as well as the ossification region in the posterior PS, and the level was decreased in mutant posterior PSs (Fig. 5D′, E′). *Loxl4* was expressed in the posterior PS ossification region as well, and expression was markedly decreased in $Yap^{fl/fl};Taz^{fl/fl};Col2^{Cre}$ embryos (Fig. 5F′, G′). Notably, family member *Loxl3* loss of function results in PS elevation delay and clefting (Zhang et al. 2015). As Loxl4 catalyzes collagen crosslinking, we measured collagen levels and found a decrease in the ossifying region in the posterior PSs in the $Yap^{fl/fl};Taz^{fl/fl};Col2^{Cre}$ mutant at E14.5 (Fig. 5H–I′). Thus, YAP/TAZ target *Ibsp* and *Phex*, which may be required for mineralization of secondary palate, and *Loxl4*, which may be required to crosslink collagen for proper PS elevation in the posterior palate.

Discussion

Here, we interrogated the involvement of YAP/TAZ in the morphogenesis of the secondary palate. We deleted *Yap*/*Taz* throughout the PS mesenchyme, or specifically in a subset of

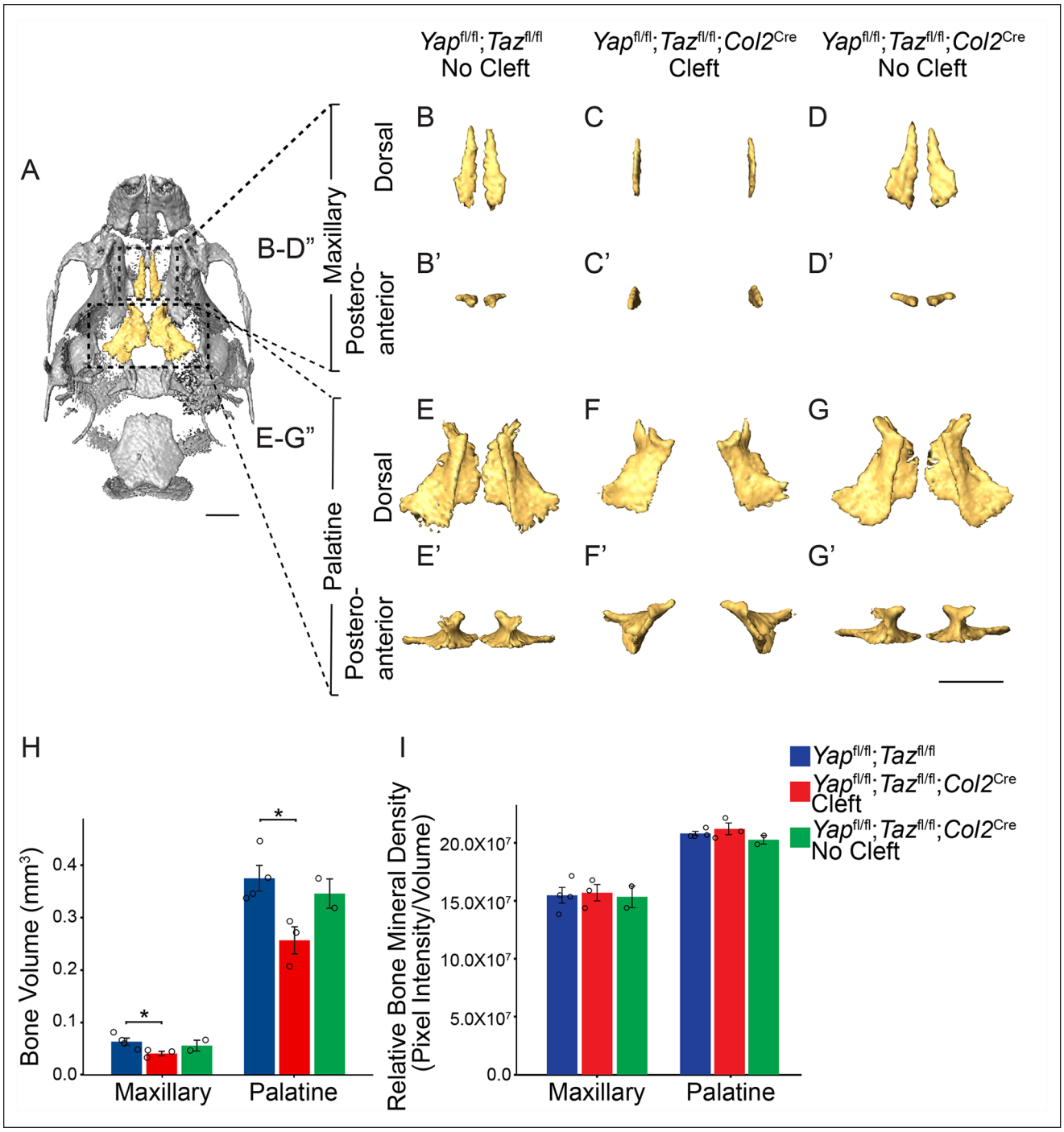

Figure 4. Deletion of *Yap*/*Taz* in the palatal shelf mesenchyme results in decreased volume of the bones of the secondary palate. (**A**) Ventral view of micro–computed tomography rendering of a E18.5 control skull with the palatine processes of the maxillary and palatine bones that compose the secondary palate false colored in yellow. (**B**–**G**′) Dorsal (B–G) and posteroanterior views (B′–G′) of segmented maxillary bone (B–D′) and palatine bone (E–G′). Note that the bones of the *Yap*$^{fl/fl}$;*Taz*$^{fl/fl}$;*Col2*^{Cre} mutant embryo were undersized and in a vertical position. Scale bar = 1 mm. (**H**) Quantification of bone volume of the maxillary and palatine bones shows decreased volume in the *Yap*$^{fl/fl}$;*Taz*$^{fl/fl}$;*Col2*^{Cre} mutants with cleft but not without cleft compared to control ($^{*}P < 0.05$). (**I**) Quantification of the relative bone mineral density shows no significant difference in bone density in the *Yap*$^{fl/fl}$;*Taz*$^{fl/fl}$;*Col2*^{Cre} mutant embryos compared to control.

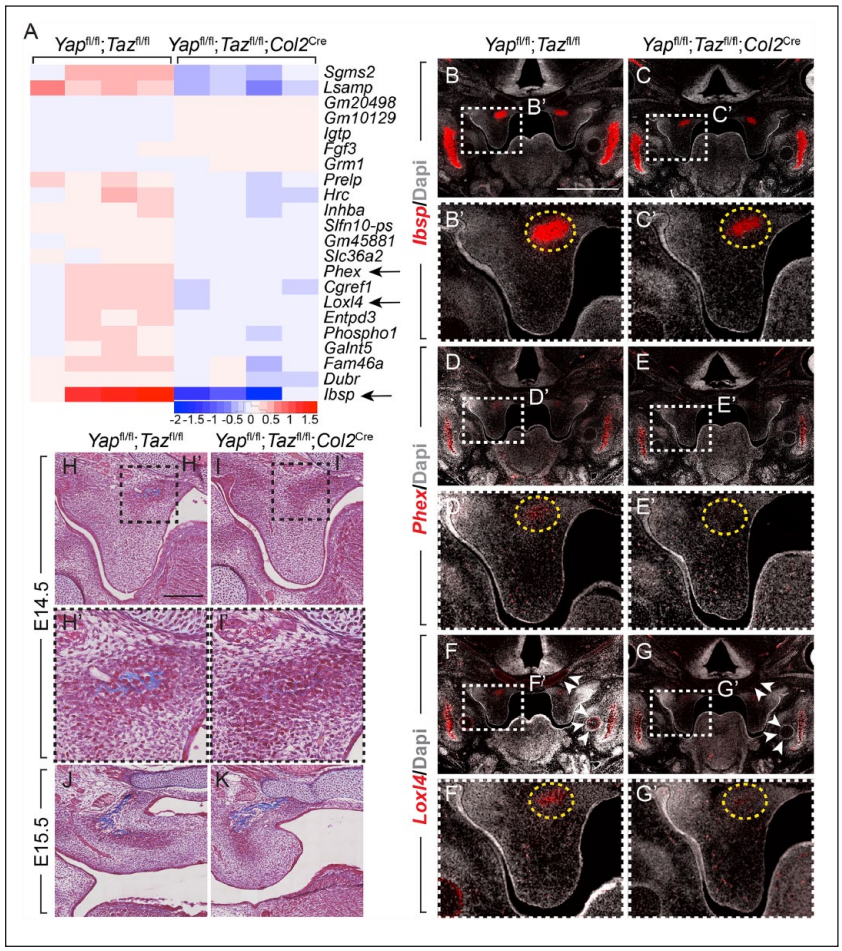

Figure 5. Yap/Taz regulate transcription of genes necessary for elevation and mineralization in the palatal shelves. (**A**) Heatmap of the 22 differentially expressed genes (false discovery rate <0.05) in nonelevated posterior palatal shelves in *Yap*$^{fl/fl}$;*Taz*$^{fl/fl}$ control and *Yap*$^{fl/fl}$;*Taz*$^{fl/fl}$;*Col2*^{Cre} mutant embryos at E14.5. Highlighted with arrows are the 3 most differentially expressed genes, *Ibsp, Phex*, and *Loxl4*. (**B–G″**) Messenger RNA levels of *Ibsp* (B–C′), *Phex* (D–E′), and *Loxl4* (F–G′) in the posterior palatal shelves in *Yap*$^{fl/fl}$;*Taz*$^{fl/fl}$ control (B, D, F) and *Yap*$^{fl/fl}$;*Taz*$^{fl/fl}$;*Col2*^{Cre} mutant (C, E, G) embryos at E14.5. *Ibsp* was expressed in the mineralizing mandible (B, C) and posterior palatal shelf mesenchyme in the ossification region, where it was decreased in the mutant compared to control (B′, C′, yellow dashed circle). *Phex* and *Loxl4* were similarly expressed in the ossification center in the posterior palatal mesenchyme and decreased in *Yap*$^{fl/fl}$;*Taz*$^{fl/fl}$;*Col2*^{Cre} mutant embryos compared to control (D′, E′, F′, G′, yellow dashed circle). *Loxl4* was also expressed in Meckel's as well as cranial base cartilages, where *Col2*^{Cre} drives recombination, and there was a decrease in *Loxl4* expression in these cartilages in the *Yap*$^{fl/fl}$;*Taz*$^{fl/fl}$;*Col2*^{Cre} embryos compared to control (F, G, white arrowheads). Scale bar = 1 mm. (**H–K**) Masson trichrome staining (blue) in the posterior palatal shelf shows decreased staining in the ossification region of the *Yap*$^{fl/fl}$;*Taz*$^{fl/fl}$;*Col2*^{Cre} mutant embryo compared to *Yap*$^{fl/fl}$;*Taz*$^{fl/fl}$ control at E14.5 (H, H′, I, I′), and staining was similar in control and mutant at E15.5 (J, K). Scale bar = 200 µm.

mesenchymal cells in the posterior PSs, using the *Osr2*^{Cre} or *Col2*^{Cre} drivers, respectively. The *Col2*^{Cre} driver has not been classically used in this context, but its specific expression in the posterior PS mesenchyme makes this driver potentially useful to the field. Loss of *Yap*/*Taz* in the PS mesenchyme resulted in a delay in PS elevation and clefting of the secondary palate. The elevation delay was intrinsic to the PSs because, although *Col2*^{Cre} is expressed in Meckel's cartilage in the mandible, there was no difference in shape of the mandible, and removal of the mandible in *Yap*$^{fl/fl}$;*Taz*$^{fl/fl}$;*Col2*^{Cre} embryos did not rescue clefting in culture. In addition, YAP/TAZ regulate *Loxl4*, which is involved in collagen crosslinking and specifically expressed in the posterior PS mesenchyme, suggesting a role in PS elevation. Furthermore, the bones of the secondary palate were smaller in the *Yap*$^{fl/fl}$;*Taz*$^{fl/fl}$;*Col2*^{Cre} embryos compared to controls, and YAP/TAZ targeted genes that are known to be involved in bone mineralization. Thus, our data show that YAP/TAZ are important in regulating both PS elevation and mineralization of the bones of the secondary palate.

PS elevation is one of the least well-understood aspects of secondary palatogenesis, and many tissue and cellular processes have been proposed to contribute to this process. Proliferation is thought to play an essential role (Lan et al. 2004; Zhou et al. 2013), and deletion of *Yap*/*Taz* with the *Osr2*^{Cre} driver led to a significant decrease in cell proliferation in the posterior PS mesenchyme. This may contribute to the elevation defect, but the proliferation decrease was relatively small, and so other mechanisms are likely involved.

For decades, it has been suggested that glycosaminoglycans (GAGs), including the predominant GAG in PS mesenchyme, hyaluronic acid (HA), play a critical role in PS elevation, because HA accumulates in the PS mesenchyme prior to elevation and binds water, which is thought to provide the intrinsic force necessary for elevation (Brinkley and Morris-Wiman 1987). More recently, deletion of *Has2*, which encodes an enzyme that catalyzes HA synthesis, resulted in elevation delay and clefting (Lan et al. 2019; Yonemitsu et al. 2020). With deletion of *Yap*/*Taz* in the PS mesenchyme with either the *Osr2*^{Cre} or *Col2*^{Cre} driver, we found no decrease in HA levels (Appendix Fig. 8A–B′), and there were no significant changes in expression of *Has1–3* in the posterior PS prior to elevation at E14.5 (Appendix Fig. 8C). Therefore, it does not appear that YAP/TAZ regulate HA synthesis or accumulation to regulate PS elevation.

Other extracellular matrix (ECM) components have been proposed to play a role in PS elevation. For example, collagens are highly organized in the PS mesenchyme prior to elevation (Chiquet et al. 2016), and collagen crosslinking is critical in PS elevation (Zhang et al. 2015). *Loxl4*, a target of YAP/TAZ, was expressed specifically in the ossification center in the superior region of the posterior PS mesenchyme. Although the contribution of this region to PS elevation is not fully understood,

ECM reorganization may generate intrinsic forces necessary for elevation in this region (Chiquet et al. 2016). Our finding that YAP/TAZ regulate *Loxl4* expression suggests that YAP/TAZ signaling and induction of *Loxl4* may be necessary for PS elevation.

Later in development, we found that YAP/TAZ play a role in mineralization of the bones of the secondary palate. There is conflicting evidence for YAP/TAZ both inhibiting and promoting osteoblast differentiation and bone formation in vitro and in vivo (Zaidi et al. 2004; Byun et al. 2014; Park et al. 2015; Kegelman et al. 2018). This phenotype may be secondary to the PS elevation delay, since we only see a decreased bone volume phenotype in the $Yap^{fl/fl}$;$Taz^{fl/fl}$;$Col2^{Cre}$ mutant embryos with clefts but not in those without. However, our RNA-seq data showed that YAP/TAZ activate genes involved in mineralization, and we observed significant reduction in mineralization in other bones of the skull that form via endochondral ossification (Appendix Fig. 7B–E and Appendix Fig. 9A–D).

Together, our data suggest that YAP/TAZ play a dual role in secondary palatogenesis, regulating PS elevation by controlling proliferation and expression of *Loxl4* in the PS mesenchyme, as well as mineralization of the bones of the secondary palate by inducing expression of *Ibsp* and *Phex*. Further investigation, including study of early morphogenesis of the palatal shelves that may contribute to the later elevation and mineralization defects, will be necessary to obtain deeper insights into these roles of YAP/TAZ in secondary palate formation.

Author Contributions

A.F. Goodwin, contributed to conception, design, data acquisition, analysis, and interpretation, drafted and critically revised the manuscript; C.P. Chen, contributed to data acquisition, analysis, and interpretation, critically revised the manuscript; N.T. Vo, contributed to data acquisition and analysis, critically revised the manuscript; J.O. Bush, O.D. Klein, contributed to conception, design, data analysis, and interpretation, drafted and critically revised the manuscript. All authors gave final approval and agree to be accountable for all aspects of the work.

Acknowledgments

This work was funded in part by the National Institute of Dental and Craniofacial Research (5K08DE028011 to A.F. Goodwin, R01DE023337 to J.O. Bush, and R01DE027620 to O.D. Klein) and the American Association of Orthodontists Foundation (Postdoctoral Fellowship Award to A.F. Goodwin). The authors declare no potential conflicts of interest with respect to the authorship and/or publication of this article.

ORCID iD

C.P. Chen https://orcid.org/0000-0002-0800-444X

References

Brinkley LL, Morris-Wiman J. 1987. Computer-assisted analysis of hyaluronate distribution during morphogenesis of the mouse secondary palate. Development. 100(4):629–635.

Brock LJ, Economou AD, Cobourne MT, Green JBA. 2016. Mapping cellular processes in the mesenchyme during palatal development in the absence of Tbx1 reveals complex proliferation changes and perturbed cell packing and polarity. J Anat. 228(3):464–473.

Brunet CL, Sharpe PM, Ferguson MW. 1993. The distribution of epidermal growth factor binding sites in the developing mouse palate. Int J Dev Biol. 37(3):451–458.

Bush JO, Jiang R. 2012. Palatogenesis: morphogenetic and molecular mechanisms of secondary palate development. Development. 139(2):231–243.

Byun MR, Hwang JH, Kim AR, Kim KM, Hwang ES, Yaffe MB, Hong JH. 2014. Canonical Wnt signalling activates TAZ through PP1A during osteogenic differentiation. Cell Death Differ. 21(6):854–863.

Chiquet M, Blumer S, Angelini M, Mitsiadis TA, Katsaros C. 2016. Mesenchymal remodeling during palatal shelf elevation revealed by extracellular matrix and F-actin expression patterns. Front Physiol. 392(7):1–13.

Coleman RD. 1965. Development of the rat palate. Anat Rec. 151(1):107–117.

Cuervo R, Covarrubias L. 2004. Death is the major fate of medial edge epithelial cells and the cause of basal lamina degradation during palatogenesis. Development. 131(1):15–24.

Dudas M, Sridurongrit S, Nagy A, Okazaki K, Kaartinen V. 2004. Craniofacial defects in mice lacking BMP type I receptor Alk2 in neural crest cells. Mech Dev. 121(2):173–182.

Dupont S, Morsut L, Aragona M, Enzo E, Giulitti S, Cordenonsi M, Zanconato F, Le Digabel J, Forcato M, Bicciato S, et al. 2011. Role of YAP/TAZ in mechanotransduction. Nature. 474(7350):179–183.

Ferguson MW. 1977. The mechanism of palatal shelf elevation and the pathogenesis of cleft palate. Virchows Arch A Pathol Anat Histol. 375(2):97–113.

Ferguson MW. 1978. Palatal shelf elevation in the Wistar rat fetus. J Anat. 125(Pt 3):555–577.

Ferguson MW. 1988. Palate development. Development. 103(Suppl):41–60.

Friedl RM, Raja S, Metzler MA, Patel ND, Brittian KR, Jones SP, Sandell LL. 2019. RDH10 function is necessary for spontaneous fetal mouth movement that facilitates palate shelf elevation. Dis Model Mech. 12(7):1–14.

Geyer SH, Reissig L, Rose J, Wilson R, Prin F, Szumska D, Ramirez-Solis R, Tudor C, White J, Mohun TJ, et al. 2017. A staging system for correct phenotype interpretation of mouse embryos harvested on embryonic day 14 (E14.5). J Anat. 230(5):710–719.

Hu JK, Du W, Shelton SJ, Oldham MC, DiPersio CM, Klein OD. 2017. An FAK-YAP-mTOR signaling axis regulates stem cell-based tissue renewal in mice. Cell Stem Cell. 21(1):91–106.e6.

Huang X, Goudy SL, Ketova T, Litingtung Y, Chiang C. 2008. Gli3-deficient mice exhibit cleft palate associated with abnormal tongue development. Dev Dyn. 237(10):3079–3087.

Jin J-Z, Tan M, Warner DR, Darling DS, Higashi Y, Gridley T, Ding J. 2010. Mesenchymal cell remodeling during mouse secondary palate reorientation. Dev Dyn. 239(7):2110–2117.

Kegelman CD, Mason DE, Dawahare JH, Horan DJ, Vigil GD, Howard SS, Robling AG, Bellido TM, Boerckel JD. 2018. Skeletal cell YAP and TAZ combinatorially promote bone development. FASEB J. 32(5):2706–2721.

Kim S, Lewis AE, Singh V, Ma X, Adelstein R, Bush JO. 2015. Convergence and extrusion are required for normal fusion of the mammalian secondary palate. PLoS Biol. 13(4):e1002122.

Lan Y, Ovitt CE, Cho E-S, Maltby KM, Wang Q, Jiang R. 2004. Odd-skipped related 2 (Osr2) encodes a key intrinsic regulator of secondary palate growth and morphogenesis. Development. 131(13):3207–3216.

Lan Y, Qin C, Jiang R. 2019. Requirement of hyaluronan synthase-2 in craniofacial and palate development. J Dent Res. 98(12):1367–1375.

Li CY, Hu J, Lu H, Lan J, Du W, Galicia N, Klein OD. 2016. αE-catenin inhibits YAP/TAZ activity to regulate signalling centre formation during tooth development. Nat Commun. 7:12133.

Liu CY, Zha ZY, Zhou X, Zhang H, Huang W, Zhao D, Li T, Chan SW, Lim CJ, Hong W, et al. 2010. The hippo tumor pathway promotes TAZ degradation by phosphorylating a phosphodegron and recruiting the SCFβ-TrCP E3 ligase. J Biol Chem. 285(48):37159–37169.

Mai CT, Isenburg JL, Canfield MA, Meyer RE, Correa A, Alverson CJ, Lupo PJ, Riehle-Colarusso T, Cho SJ, Aggarwal D, et al. 2019. National population-based estimates for major birth defects, 2010–2014. Birth Defects Res. 111(18):1420–1435.

Mansell JP, Kerrigan J, McGill J, Bailey J, TeKoppele J, Sandy JR. 2000. Temporal changes in collagen composition and metabolism during rodent palatogenesis. Mech Ageing Dev. 119(1–2):49–62.

Morris-Wiman J, Brinkley L. 1993. Rapid changes in the extracellular matrix accompany in vitro palatal shelf remodelling. Anat Embryol (Berl). 188(1):75–85.

Nagata M, Ohashi Y, Ozawa H. 1991. A histochemical study of the development of premaxilla and maxilla during secondary palate formation in the mouse embryo. Arch Histol Cytol. 54(3):267–278.

Parada C, Han D, Grimaldi A, Sarrión P, Park SS, Pelikan R, Sanchez-Lara PA, Chai Y. 2015. Disruption of the ERK/MAPK pathway in neural crest cells as a potential cause of Pierre Robin sequence. Development. 142(21):3734–3745.

Park HW, Kim YC, Yu B, Moroishi T, Mo J-S, Plouffe SW, Meng Z, Lin KC, Yu F-X, Alexander CM, et al. 2015. Alternative wnt signaling activates YAP/TAZ. Cell. 162(4):780–794.

Richardson RJ, Dixon J, Jiang R, Dixon MJ. 2009. Integration of IRF6 and Jagged2 signalling is essential for controlling palatal adhesion and fusion competence. Hum Mol Genet. 18(14):2632–2642.

Shiota K, Kosazuma T, Klug S, Neubert D. 1990. Development of the fetal mouse palate in suspension organ culture. Acta Anat (Basel). 137(1):59–64.

Vassilev A, Kaneko KJ, Shu H, Zhao Y, DePamphilis ML. 2001. TEAD/TEF transcription factors utilize the activation domain of YAP65, a Src/Yes-associated protein localized in the cytoplasm. Genes Dev. 15(10):1229–1241.

Wada K-I, Itoga K, Okano T, Yonemura S, Sasaki H. 2011. Hippo pathway regulation by cell morphology and stress fibers. Development. 138(18):3907–3914.

Walker BE, Fraser FC. 1956. Closure of the secondary palate in three strains of mice. J Embryol Exp Morphol. 4(Pt 2):176–189.

Wang J, Xiao Y, Hsu C-W, Martinez-Traverso IM, Zhang M, Bai Y, Ishii M, Maxson RE, Olson EN, Dickinson ME, et al. 2016. Yap and Taz play a crucial role in neural crest-derived craniofacial development. Development. 143(3):504–515.

Williamson KA, Rainger J, Floyd JAB, Ansari M, Meynert A, Aldridge KV, Rainger JK, Anderson CA, Moore AT, Hurles ME, et al. 2014. Heterozygous loss-of-function mutations in YAP1 cause both isolated and syndromic optic fissure closure defects. Am J Hum Genet. 94(2):295–302.

Yonemitsu MA, Lin TY, Yu K. 2020. Hyaluronic acid is required for palatal shelf movement and its interaction with the tongue during palatal shelf elevation. Dev Biol. 457(1):57–68.

Yu FX, Zhao B, Guan KL. 2015. Hippo pathway in organ size control, tissue homeostasis, and cancer. Cell. 163(4):811–828.

Yu K, Ornitz DM. 2011. Histomorphological study of palatal shelf elevation during murine secondary palate formation. Dev Dyn. 240(7):1737–1744.

Yu K, Yonemitsu MA. 2019. In vitro analysis of palatal shelf elevation during secondary palate formation. Anat Rec (Hoboken). 302(9):1594–1604.

Zaidi SK, Sullivan AJ, Medina R, Ito Y, van Wijnen AJ, Stein JL, Lian JB, Stein GS. 2004. Tyrosine phosphorylation controls Runx2-mediated subnuclear targeting of YAP to repress transcription. EMBO J. 23(4):790–799.

Zhang J, Yang R, Liu Z, Hou C, Zong W, Zhang A, Sun X, Gao J. 2015. Loss of lysyl oxidase-like 3 causes cleft palate and spinal deformity in mice. Hum Mol Genet. 24(21):6174–6185.

Zhao B, Li L, Tumaneng K, Wang CY, Guan KL. 2010. A coordinated phosphorylation by Lats and CK1 regulates YAP stability through SCF(beta-TRCP). Genes Dev. 24(1):72–85.

Zhao B, Ye X, Yu J, Li L, Li W, Li S, Yu J, Lin JD, Wang CY, Chinnaiyan AM, et al. 2008. TEAD mediates YAP-dependent gene induction and growth control. Genes Dev. 22(14):1962–1971.

Zhou J, Gao Y, Lan Y, Jia S, Jiang R. 2013. Pax9 regulates a molecular network involving Bmp4, Fgf10, Shh signaling and the Osr2 transcription factor to control palate morphogenesis. Development. 140(23):4709–4718.